

Arpad A. Vass,¹ Ph.D.; Stacy-Ann Barshick,² Ph.D.; Gary Segal,³ Ph.D.; John Caton,³ Ph.D.; James T. Skeen,⁴ A.S.; Jennifer C. Love,⁵ Ph.D. and Jennifer A. Synsteliien,⁶ B.A.

Decomposition Chemistry of Human Remains: A New Methodology for Determining the Postmortem Interval*

REFERENCE: Vass AA, Barshick S-A, Segal G, Caton J, Skeen JT, Love JC, Synsteliien JA. Decomposition chemistry of human remains: a new methodology for determining the postmortem interval. *J Forensic Sci* 2002;47(3):542-553.

ABSTRACT: This study was conducted to characterize the chemistry associated with the decomposition of human remains with the objective of identifying time-dependent biomarkers of decomposition. The purpose of this work was to develop an accurate and precise method for measuring the postmortem interval (PMI) of human remains. Eighteen subjects were placed within a decay research facility throughout a four-year time period and allowed to decompose naturally. Field autopsies were performed and tissue samples were regularly collected until the tissues decomposed to the point where they were no longer recognizable (encompassing a cumulative degree hour (CDH) range of approximately 1000 (~3 weeks)). Analysis of the biomarkers (amino acids, neurotransmitters, and decomposition by-products) in various organs (liver, kidney, heart, brain, muscle) revealed distinct patterns useful for determining the PMI when based on CDHs. Proper use of the methods described herein allow for PMIs so accurate that the estimate is limited by the ability to obtain correct temperature data at a crime scene rather than sample variability.

KEYWORDS: forensic science, postmortem interval, time since death determinations, tissue composition, biomarkers

Human decomposition begins approximately 4 min after death. The onset of decomposition is governed by a process called autolysis or self digestion. As cells of the body are deprived of oxygen, carbon dioxide in the blood increases, pH decreases, and wastes accumulate, which poisons the cells. Concomitantly, cellular enzymes (lipases, proteases, amylases, etc.) begin to dissolve the cells from the inside out, eventually causing them to rupture, releasing nutrient-rich fluids. This process begins sooner and progresses

more rapidly in tissues that have a high enzyme content (such as the liver) and a high water content (such as the brain), but eventually affects all the cells in the body. Autolysis usually does not become visually apparent for a few days. It is first observed by the appearance of fluid filled blisters on the skin and skin slippage where large sheets of skin slough off the body. Meanwhile, the body has acclimated to ambient temperature (algor mortis), blood has settled in the body causing discoloration of the skin (livor mortis), and cellular cytoplasm has gelled due to increased acidity (rigor mortis) (1). After enough cells have ruptured, nutrient-rich fluids become available and the process of putrefaction can begin.

Putrefaction is the destruction of the soft tissues of the body by the action of microorganisms (bacteria, fungi, and protozoa) and results in the catabolism of tissue into gases, liquids, and simple molecules. Usually the first visible sign of putrefaction is a greenish discoloration of the skin due to the formation of sulfhemoglobin in settled blood. The process progresses into distension of tissues due to the formation of various gases (hydrogen sulfide, carbon dioxide, methane, ammonia, sulfur dioxide, and hydrogen), especially in the bowels. This is associated with anaerobic fermentation, primarily in the gut, releasing by-products rich in volatile fatty acids, primarily butyric and propionic acids. Gas and fluid accumulation in the intestines usually purge from the rectum, but can be severe enough to rip apart the skin causing additional post-mortem injuries. Shortly after the purging of gases due to putrefaction, active decay begins (1,2). Muscle, composed of protein, which in turn is composed of amino acids, readily decomposes to form additional volatile fatty acids through bacterial action. Further protein and fat decomposition yields phenolic compounds and glycerols. Compounds including indole, 3-methyl indole (skatole), putrescine, cadaverine, and various fatty acids have been detected and are significant decomposition products. At this point in the decay cycle, electrolytes are rapidly leaching out of the body, both aerobic and anaerobic bacteria are present in large numbers, insect activity is very prominent and carnivores can contribute significantly to the decline of the corpse.

Decomposition is a complicated process, but is primarily dependant on temperature, and to a lesser extent on moisture, and is the result of a complex assortment of processes ranging from enzymatic digestion and bacterial action to environmental conditions. Currently, however, there are few scientific methods based on chemical measurements that can be used to provide postmortem interval (PMI) information. Typically, such information is gained through the cooperation of trained forensic scientists who provide

¹Research Scientist, Life Sciences Division, ²Research Scientist, ³Senior Research Scientist, and ⁴Research Technician, respectively, Chemical and Analytical Sciences Division, Oak Ridge National Laboratory, Oak Ridge, TN.

⁵Forensic Anthropology Consultant, Regional Forensic Center, Memphis, TN.

⁶Graduate student, University of Tennessee, Department of Anthropology, Knoxville, TN.

Received 1 Aug. 2001; and in revised form 3 Oct. 2001; accepted 8 Oct. 2001.

*The submitted manuscript has been authorized by a contractor of the U.S. Government under contract No. DE-ACO5-84OR21400. Accordingly, the U.S. Government retains a nonexclusive, royalty-free license to publish or reproduce the published form of this contribution, or to allow others to do so, for U.S. Government purposes.

information based on experience and opinion. For example, estimating the PMI prior to the onset of putrefaction (36–72 h) generally involves visual inspection of the body by observing the appearance (i.e., rigor and livor mortis) and determining the core body temperature and gastric contents (3). During this time period, changes in blood and cerebrospinal fluid biochemistry are determined, but these measurements are subject to considerable error and are often unreliable for determining the PMI. The most accurate biochemical indicator of PMI prior to putrefaction is the potassium content of the vitreous humor (3).

To date, volatile fatty acids have been the only reliable biomarkers of PMI (4) for pre-skeletonized remains during putrefaction. The decay rate of DNA in ribs has also been investigated but has yet to be field-tested (5). The reported accuracy of the fatty acid determination method for PMI of pre-skeletonized remains is ± 2 days. Once a corpse is skeletonized, the concentrations of inorganic species (K^+ , Ca^{2+} , Mg^{2+} , etc.) that migrate into the soil from cellular constituents or skeletal material have been used for determining PMI (4). The reported accuracy of this method for PMI of skeletonized remains over a year old is ± 2 weeks. Forensic entomology is another useful tool that has, in the last several years, gained success in determining PMI (6–9) and along with decomposition by-products, is currently one of the best means of determining the PMI.

In an effort to obtain even more precise PMI estimates, the objective of this study was to identify biomarkers in various organs of the body (heart, lung, brain, kidney, liver, and muscle) associated with early decomposition of human remains. Bodily fluids were not targeted because of their reported variability (3) and inherent blending as decomposition progresses. Living matter is largely composed of water with nearly all of the organic matter consisting mainly of the elements C, H, O, N, P, and S (10). These elements combine to form the four major classes of biological macromolecules found in living matter: proteins, nucleic acids, polysaccharides, and lipids. Most of these macromolecules are composed of the various building-block molecules, which include amino acids (for proteins), nitrogenous bases, phosphate, and sugars (for nucleic acids), palmitic, and oleic acids (for lipids), and glucose (for polysaccharides) (10). It is speculated that in decomposition, as in the process of catabolism, these large biomolecules are broken down into their building-block compounds and the rate of this process may be used as a measure of PMI. Therefore, it was these building-block molecules and their degradation products that were targeted in this study. The expected products included simple sugars, aldehydes, ketones, amino acids, amines, phenolic compounds, nitrogenous bases, phosphates, fatty acids, glycerol, and sterols. As this study progressed, it became obvious that lung tissue degraded much too rapidly and contained too large a resident microbial population to be useful and was subsequently dropped from this study. During the course of this study, the initial list of biomarkers considered potentially useful for PMI determinations was narrowed to include amino acids, amines (putrescine and cadaverine), and carboxylic acids—gamma-aminobutyric acid (GABA) and gamma-hydroxybutyric acid (GHB). Only these compounds met our criteria as possible biomarkers: a) reproducible—within tissues (less than 10% variability) and between corpses, and b) concentrations high enough to allow for consistent detection and evaluation of reproducibility.

Materials and Methods

A total of eighteen unembalmed, unautopsied cadavers were placed at the University of Tennessee's Forensic Anthropology Re-

search Center (FARC) during various seasons over a four-year time period. This facility is located in a secluded, open-wooded area in Knoxville, Tennessee, dedicated to the study of the decomposition of human remains in a natural environment. This 2+ acre facility is surrounded by a chain-link fence to restrict large carnivores and is under 24 h surveillance to prevent unauthorized intrusions.

The subjects were stored in morgue coolers or came directly from funeral homes prior to the onset of the decay study. Information concerning the race, age, gender, sampling method, and cause of death was recorded for all individuals, if available (Table 1). Sufficient subjects were available in order to incorporate as many variables into this study as possible. These included decomposition while clothed vs. unclothed, in polyethylene body bags vs. surface decomposition, and fresh vs. aged in morgue coolers. Data concerning climatic conditions (temperature, humidity, and rainfall) were collected using an electronic weather station (VWR Scientific) in the vicinity of the sampling area. The state of decomposition and insect activity were also recorded at each sampling.

Tissue samples were collected at various intervals spanning from twice a day to up to six days between samplings. Photographs of selected corpses were also taken at the time of sampling for future reference.

Subject Selection

The bodies used in this study were donations to the Forensic Anthropology Research Center at the University of Tennessee in Knoxville. The individuals had either voluntarily donated their remains to the center for research purposes, had signed papers to donate their remains to science, or had been donated by family members.

Individuals were selected based on: a) having a known perimortem interval; b) having a known ambient air temperature record after death; c) having a known cause of death; and d) being unautopsied. Individuals having known blood borne pathogens were excluded from this study. Additionally, only individuals who either exhibited no gross external decompositional changes or were in the early stages of decomposition (i.e., abdominal discoloration, slight bloating and/or livor or rigor mortis) were used for this study.

Tissue Sampling Procedure

Tissues collected were brain, heart, lung, liver, kidney, and muscle. Two methods of tissue sampling were employed. At the onset of the project, our goal was to keep external bacterial and insect invasion of the tissue at a minimum. As a result, we wanted to minimize the size of the entry wound. For this reason, we employed a probe method of tissue sampling. Five individuals were sampled using a Bauer Temno automatic, one-hand operation biopsy needle. The skin was punctured with the needle and a biopsy obtained. Due to the difficulty involved in locating and isolating the tissue, the biopsy needle approach was discontinued. Instead, the body cavities were accessed through scalpel incisions and a 1 to 2 gram bulk tissue sample was excised using tissue forceps and dissection scissors (refer to Table 1). Brain tissues were obtained by either the biopsy needle or with a Lawson tissue biopsy forcep.

The thoracic cavity was accessed through a modified "Y" shaped incision made with a scalpel. The arms of the Y were formed by diagonal incisions that began just below each clavicle and extended to the suprasternal notch. A midline vertical incision from the suprasternal notch to just below the xiphoid process of the sternum formed the body of the Y. Two more diagonal incisions were then made, which extended along the costal margins of the rib cage bi-

TABLE 1—Summary of available information on test subjects.

Subject	Gender	Race	Age	Sampling Method	Cause of Death	In Morgue Cooler Prior to Study	Decomposition in Body Bag	Comments
1	F	C	73	Bulk	Lung cancer	No	No	Heavy smoker
2	F	C	53	Bulk	ASCVD	1 day	No	Amputated leg, by-pass surgery 7 days prior to death
3	F	C	70	Bulk	Acute abdomen perforated bowel	No, on dry ice during shipment to FARC	No	Post polio syndrome, anemia, systemic sclerosis
4	M	C	57	Bulk	ASCVD	6 days	Yes	
5	M	C	97	Bulk	Pneumonia	No	No	
6	M	C	78	Bulk	Unspecified natural causes	No	No	
7	F	C	94	Bulk	Cancer	No	No	
8	M	C	58	Bulk	Unspecified natural causes	21 days	Yes	Gout, epilepsy
9	M	C	89	Bulk	ASCVD	4 days	Yes	
10	M	C	79	Probe	CVA/ASCVD	1 day	No	Diabetic, both legs amputated
11	M	C	65	Bulk	Respiratory failure	No	No	Lymphoma
12	M	C	88	Probe	Blunt force head trauma	No	No	Decomposed fully clothed
13	F	C	67	Probe	Cancer	No	No	
14	F	C	67	Probe	Malnutrition, heart and respiratory failure	No	No	Anemia, emaciated, abdominal surgery
15	M	C	85	Probe	ASCVD	2 days	No	Emaciated
16	F	C	43	Bulk	Cocaine toxicity	6 days	Yes	
17	M	C	61	Bulk	Asbestosis +	1 day	Yes	
18	F	C	34	Bulk	Ethanol cyclobenzaprine toxicity	26 days	Yes	

C - Caucasian, ASCVD - atherosclerosis cardiovascular disease, CVA - cerebrovascular accident. FARC - Forensic Anthropology Research Center.

laterally, resulting in the formation of two skin flaps. The skin flaps were then dissected off the rib cage and a scalpel blade and/or metacarpel saw was used to cut through the costal cartilage. The sterno-clavicular joints were kept intact so that the chest plate (plastron) could be lifted up and held in place while the thoracic cavity was accessed. The myocardium of the left ventricle of the heart was sampled. Heart tissue sampling was discontinued either due to lack of myocardium tissue, gross morphological tissue degradation, or extensive maggot invasion. Lung samples were obtained from the anterior surface of either lung. Sampling of the lung was discontinued either due to tissue liquefaction or extensive maggot invasion. After the organs were sampled, the sternum was replaced, the skin flaps joined together and duct tape placed over the incisions.

The abdominal cavity was accessed through a "V" shaped incision made with a scalpel on the right side of the abdomen. One arm of the V was formed by an incision that extended from just below the costal cartilage of the eighth rib to the right lower quadrant (RLQ) of the abdomen. The V was then completed by a diagonal incision from the RLQ to the mid-epigastric region of the abdomen. Care was taken to avoid puncturing the intestines. The location of the liver sample was randomly selected, but in most cases was obtained from the anterior portion of the right lobe. Sampling of the liver ended when the tissue was either near liquefaction or had extensive maggot invasion. The location of the kidney sample was randomly selected. For individuals having a relatively small kidney, an additional V incision was made on the left side of the abdomen and the second kidney sampled to extend the sampling interval. The kidney was sampled until no more tissue could be obtained due to either lack of tissue, extensive maggot activity, or extensive intestinal bloating that rendered the tissue inaccessible.

The cranial cavity was accessed by puncturing a hole large enough to allow the biopsy needle, or forceps, to pass through the

posterior of the orbit near, or at the superior orbital fissure. In some instances, the eye was enucleated for easier access to the brain. Brain tissue was collected from the frontal and/or parietal lobes of the cerebrum. This collection technique was utilized in order to preserve the cranium for the anthropological skeletal research collection at the University of Tennessee.

Random muscle samples were obtained from the quadriceps through an approximately 5 cm long vertical incision on the anterior thigh. The incision was then covered with duct tape and in subsequent samplings muscle was obtained through the same incision until the tissue began to show gross morphological color changes. New incisions were then made along the anterior thigh as needed until sampling could no longer continue due to either the absence of muscle tissue, or extensive maggot activity. For some of the earlier individuals in the study, muscle tissue was randomly sampled from the biceps, pectoralis, abdominal, calf, or quadriceps muscles.

After tissue sampling, all incisions were sealed with duct tape to prevent fly and subsequent maggot invasion of the body cavities. Once maggot invasion could no longer be prevented, the duct tape was permanently removed and the incisions were left exposed.

Tissue Storage

All tissue samples were placed in plastic vials inside Ziploc freezer bags and stored in a freezer maintained at -80°C until processing.

Sample Processing

All tissue samples were processed in a similar fashion. While still frozen, all obvious fatty deposits were removed from the surface of the organ samples. Small sections of tissue were then cut from the bulk sample. No attempt was made to remove surface ma-

terial from the bulk sample prior to its dissection. Cut sections were then weighed using a Mettler AE 50 balance and sufficient material collected to obtain 100 to 200 mg of sample. This material was placed in an ice-chilled tissue grinder (VWR Scientific) and the volume adjusted to 1.5 mLs using an ice-chilled 10 mM ethylenediamine tetraacetic acid (EDTA) buffer solution. The material was hand ground (with constant re-chilling on ice) until the tissue was completely macerated. The material was then removed and placed in a 2 mL polypropylene centrifuge tube and centrifuged at 13 000 x g for 30 min (Chemle Z231 M). Centrifugation took place in a refrigerator held at 4°C. After centrifugation, the supernate was carefully removed and placed in another polypropylene centrifuge tube. This sample was then stored in a refrigerator (4°C) before derivatization. This sample was not frozen since it was observed that a permanent precipitate formed when the liquid was frozen.

Derivatization

All samples were derivatized in order to increase their volatility, thermal stability, and mass spectral detection (11). Two separate derivatizations were utilized, one for the amino acid series and one for putrescine and cadaverine. Twenty μL of the sample homogenates were pipetted into 0.3 mL Reacti-Vials (Pierce, Rockford, Illinois) and dried with low heat (40°C) under a constant stream of nitrogen.

Amino Acids were derivatized (t-BDMS derivatized) by adding 10 μL of pyridine + 10 μL (N-methyl-N-[t-butyl-dimethylsilyl]-trifluoroacetamide) (MTBSTFA) (Aldrich Chem Co., Milwaukee, Wisconsin) to the dried sample and the vial was tightly sealed. The sample was then heated to 80°C in a heating block for 30 min with several vortexings and allowed to cool before transfer to an autosampler vial for analysis. Dilutions, if needed, were made with pyridine (typically liver samples were very concentrated and began overloading the column and were the only organ samples requiring further dilution).

Cadaverine and putrescine in the dried samples were methylated by adding 10 μL of pyridine + 10 μL Methyl-8® (DMF Dimethyl acetal) (Pierce, Rockford, Illinois) and heated at 80°C for 40 min with several vortexings. After cooling, all samples were diluted with 80 μL toluene. The supernate was recovered and the sample was transferred to an autosampler vial for analysis. If the samples were too concentrated and began overloading the column, additional dilutions were made with toluene.

Amino acid, oxalic acid, putrescine, and cadaverine standards (10 to 100 ppm) were prepared in the laboratory and derivatized in a manner identical to the samples.

Sample Analysis

Samples were analyzed by gas chromatography/mass spectrometry (GC/MS) with a Hewlett Packard 5890 Series II Gas Chromatograph coupled to a HP5989A MS Engine. An autosampler (HP7673) was also utilized. The MS Engine was operated under the following conditions: Ionization Mode—Electron Impact, Polarity—Positive, Filament Emission Current—300 μA , Electron Energy—70 eV, MS Source Temperature—174°C, MS Quad Temperature—100°C, Scanned 35–550 AMU at 1 scan/s.

Both of the methods (Putrescine/Cadaverine and Amino Acids) were developed using splitless injection. The split valve was always turned on at 2 min after sample injection. The split vent flow rate was set at 16 mL/min. The injection volume was 1 μL . The GC column used was a J&W DB-5MS, 30m long with a 0.25 mm O.D. and a 0.25 micron film thickness. The HP5890 GC was operated

under the following conditions: Injection Port Temperature—175°C, Transfer Line Temperature—280°C, Column Head Pressure—15 p.s.i., Putrescine/Cadaverine GC Program—Start at 100°C—Hold 4 min—Ramp to 280°C at 10°C/min—hold 4 min., Putrescine/Cadaverine Method Solvent Delay—10 min, Amino Acids GC Program - Start at 100°C—Hold 4 min—Ramp to 280°C at 5°C/min.—hold 5 min Amino Acids Method Solvent Delay—12 min.

All data analysis was performed on HP Chemstation Software (version B.02.05). A 3-point external standard calibration was used to quantitate the putrescine/cadaverine samples, and a 4-point calibration was used for the amino acids. Quantitation was performed by integrating the area of a single ion in the compound of interest and determining the concentration from the calibration curve.

Cumulative Degree Hours (CDH)

Accumulated Degree Days (ADDs), as described by Edwards et al. (12), have typically been used for PMI determinations and are determined by taking the sum of the average daily temperatures (°C) for however long the corpse has been decomposing. For example, one subject may require 4 days (assuming an average daily temperature of 25°C) to attain an ADD score of 100, while another subject, decomposing under cooler temperatures, may also obtain an ADD score of 100, but which would require 20 days (assuming a daily average temperature of 5°C) to attain the same decompositional status and hence the same ratios of biomarkers in specific tissues. This study indicates that ADDs are no longer sufficient to accurately describe the narrowing PMIs. A more accurate technique, based on ADDs, is the use of cumulative degree hours (CDHs). This uses a twelve hour temperature cycle to describe the decompositional process. Instead of using daily average temperatures, the average temperature (°C) for each twelve hour interval is cumulatively added to attain the CDH. For example, if maximum temperature (30°C) is reached at noon every day and minimum temperature (10°C) is reached every day at midnight, then in a 24 h period (one day) the CDH would be 40 CDHs ($(30 + 10)/2 = 20$ for the first 12 h — noon to midnight and $(10 + 30)/2 = 20$ from midnight to noon for the second twelve h interval resulting in $20 + 20 = 40$ CDHs).

Because of the increased salt concentrations in the human body, decomposition still occurs when the temperature falls to 0°C. For this reason, any CDHs below 0°C are counted as zero and not as a negative number in order to avoid subtracting hours from the PMI estimate. Maximum and minimum temperatures from an actual crime scene can be obtained from the nearest National Weather Service (NWS) Station. These values can then be corrected to account for temperature variations by monitoring the maximum and minimum temperatures at the crime scene for several days and comparing them to the NWS values.

Empirical Model Design

The PMI model displayed as linked boxes in Figs. 1 to 5 was derived empirically. The model was difficult to develop because of the large variability (absolute concentrations) observed across subjects, the result of inherent differences among subjects and the differing environmental conditions not fully attributable to CDH. Although there is large variability among subjects, there were consistent patterns (compositional changes) of biomarker relationships that persisted across the entire set of subjects. These patterns are the basis of the PMI model. Decisions taken in the PMI flow charts (Figs. 1 to 5) result in refined CDH predictions. A predicted CDH range is the range of CDHs derived from subjects satisfying

the inequalities in a box and all boxes linked to it from above. Linear interpolation was used to calculate individual subjects' CDH when the exact CDH was not observed.

Results

The initial results of this study demonstrated that one particular compound, oxalic acid, is an important determinant, which affects PMI decisions. This compound was not initially targeted as important in PMI determinations, but was discovered incidentally. Oxalic acid derivatizes easily and is readily detectable in even the earliest tissue samples with a characteristic molecular ion of $m/z = 261$ (Fig. 1). This compound, given time, then goes through a reduction reaction, apparently converting a $C = O$ group to a methylene group producing an oxalic acid derivative with a molecular ion at $m/z = 247$ (Fig. 2) and was subsequently identified as hydroxyacetic acid (glycolic acid). This reduction reaction occurs at different times (CDHs) depending on the tissue type (Table 2) and is an informative PMI indicator by itself. Since glycolic acid nearly co-elutes with oxalic acid, (differentiation based on area integration

using either ions 261 or 247; Figs. 1, 2, and 3) the oxalic acid abundance is determined as a combination of both forms unless otherwise indicated.

Other important compound ratios, which have been found to be reproducible between corpses, include a variety of amino acids and gamma amino butyric acid (GABA). In order for a compound to be relevant for PMI determinations in this study, its ratio compared to other biomarkers must be reproducible over time. Absolute concentrations fluctuated dramatically from corpse to corpse and could not be used in this context. Since varying biomarkers became relevant depending on the tissue type, tissues could not be compared to

TABLE 2—Appearance of glycolic acid in different tissues.

Organ	Muscle	Liver	Heart	Kidney	Brain
CDH	350	~250	~160	~220	115

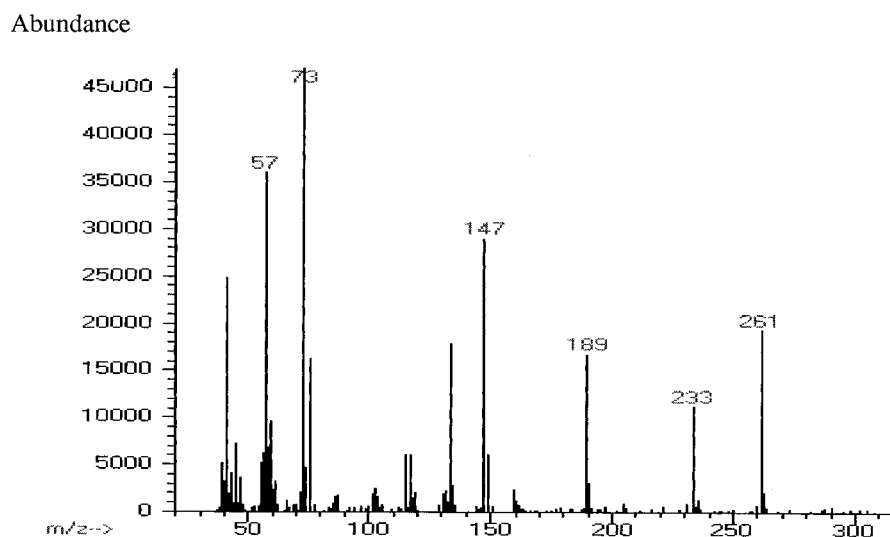


FIG. 1—Mass spectrum of oxalic acid (t -BDMS reacted).

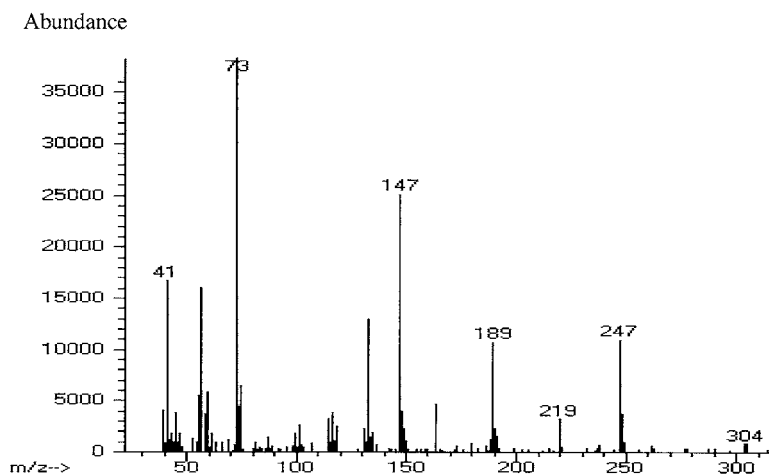


FIG. 2—Mass spectrum of the oxalic acid reduction product - glycolic acid (t -BDMS reacted).

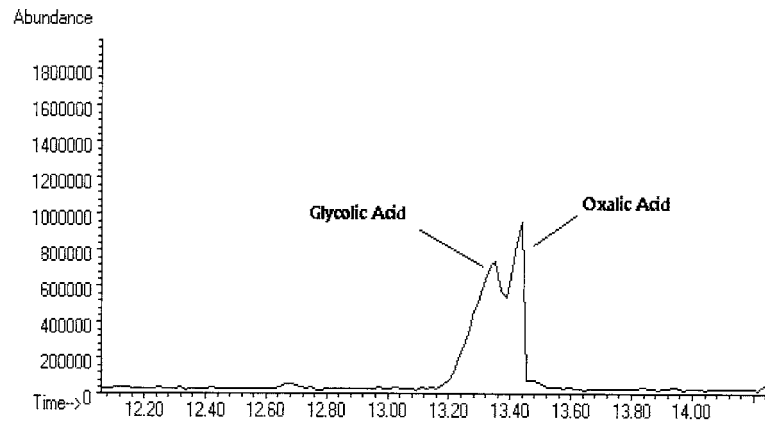


FIG. 3—Total ion current plot showing near co-elution of oxalic acid and its reduction product (glycolic acid).

TABLE 3—Important tissue biomarkers for PMI determinations and their CDH ranges.

Biomarker	Liver (0–828)	Kidney (0–970)	Heart (0–608)	Brain (0–270)	Muscle (0–798)
Alanine		519–970	0–608		401–798
Aspartate			0–165	66–114	526–798
Cysteine	0–98		166–255		
GABA	0–828	0–970	166–608	0–50	351–798
Glutamate	0–98		256–420		
Glutamine	0–250				
Glycine	251–828				
Histidine			0–165	141–270	
Isoleucine		260–970		115–270	0–350
Leucine		0–260	466–608		0–350
Methionine	121–250	0–180	0–60	0–114	401–470
			166–608		
Oxalic acid	609–828	519–600	0–608	0–270	401–798
Phenylalanine	609–828		0–60	66–114	526–798
Proline	0–828	260–518	421–608	0–50	351–798
Serine	121–250	0–180	421–608		401–525
Threonine	401–828	0–260			
		301–518			
Tyrosine				141–270	
Valine	251–400		166–420		

each other, but become extremely important when comparing and narrowing CDH ranges for PMI determinations.

The only biomarkers investigated which had no importance in PMI determinations (because of their variability) in any of the tissues studied in this research included asparagine, tryptophan, lysine, putrescine, cadaverine, and gamma hydroxybutyric acid (GHB). Contrary to these biomarkers, GABA, proline, methionine, and oxalic acid were important PMI components in all tissues studied (Table 3).

Liver

Liver tissue, along with brain, is the most diagnostic PMI indicator for early decomposition and is in general one of the best overall organs to use for PMI determinations. As with most of the organs studied, the CDH ranges of the biomarkers increase with time (PMI). The formation of the oxalic acid derivative is not as definitive in liver as in other organs and was not used as the primary determinant for PMIs. Amino acids identified as useful PMI indicators include glutamate, glutamine, proline, threonine, pheny-

lalanine, cysteine, aspartate, methionine, valine, serine, and glycine. GABA and oxalic acid have also been identified as critical markers. (Fig. 4 and Table 3).

Kidney

The kidney is a very useful organ for determining late PMIs. While early CDH ranges are not as narrow as in liver tissue, kidney has the advantage of providing CDH range information for a longer time period (up to 970 CDH), although the ranges tend to be larger the higher the CDH. Amino acids identified as useful PMI indicators include alanine, methionine, serine, isoleucine, threonine, proline and leucine. GABA and oxalic acid have also been identified as critical markers. (Fig. 5 and Table 3).

Heart

Heart tissue, like liver and brain, provides narrower CDH ranges during early decomposition. This organ provides excellent intermediate CDH ranges and is quite useful if no other organs are available for sampling. Amino acids identified as useful PMI indicators

include alanine, methionine, serine, histidine, aspartate, leucine, phenylalanine, glutamate, proline, cysteine, and valine. GABA and oxalic acid have also been identified as critical markers as was the case in the other tissues. (Fig. 6 and Table 3).

Brain

Brain tissue, while important in early CDH ranges, has limited use for long term PMI determinations since the effective CDH range only extends to approximately 270 CDHs. Glycolic acid appeared in a very narrow PMI range and was used as the definitive initial indicator. Amino acids identified as useful PMI indicators include methionine, aspartate, isoleucine, phenylalanine, tyrosine, histidine, and proline. GABA has been identified as one of the critical markers in brain tissue for early CDH ranges (Fig. 7 and Table 3).

Muscle

Surprisingly, muscle tissue has very little value in determining PMIs below 350 CDH. All amino acids, while constantly changing, tend to follow nearly identical shifts, thereby making them ineffective biomarkers. Isoleucine and leucine become important biomarkers at approximately 300 CDHs with methionine, alanine,

proline, phenylalanine, aspartate, and serine becoming important at later CDHs. The effective PMI range of muscle tissue is 800 CDH whereupon all amino acid levels tend to drop uniformly. As in all tissues examined, GABA and oxalic acid are critical biomarkers for muscle as well. (Fig. 8, Table 3).

Discussion

The appearance of glycolic acid is one of the key features of this PMI model. Oxalic acid has not been previously reported as being a major component of human tissue. It is present primarily in plants and vegetables, most notably in those of the Oxalis and Rumex families (13), where it occurs in the cell sap. It is also a product of the metabolism of many molds that convert sugar to potassium or calcium oxalate. Since oxalic acid was detectable in even the earliest samples obtained in this study, it is hypothesized that oxalic acid is derived from the enzymatic breakdown of oxaloacetic acid (a key molecule of the Krebs cycle) into oxalic acid and acetic acid. Acetic acid has been previously detected as a decomposition by-product in human decomposition (4). While the mechanism of conversion of oxalic acid to glycolic acid is unknown, it is postulated that enzymes produced from molds may play a role in this conversion (13). Additional experiments where oxalic acid was added to

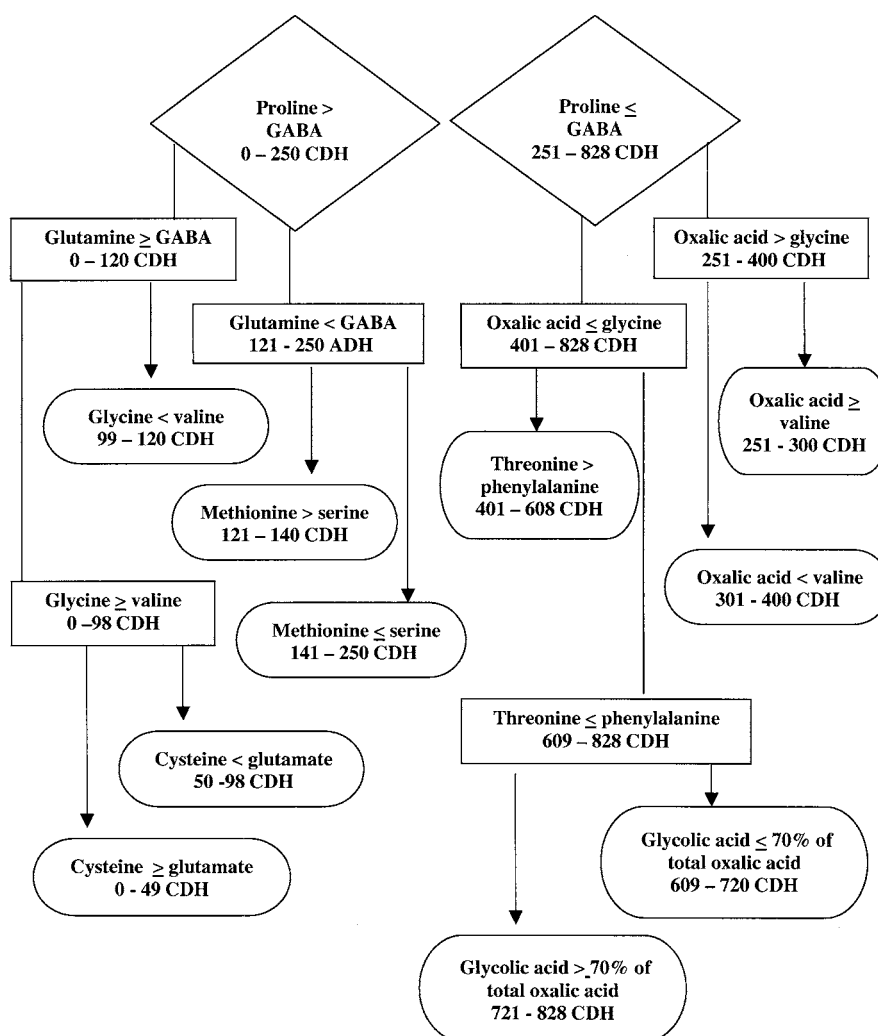


FIG. 4—Liver (Potential CDH Range 0–828).

tissue extracts (>300 CDHs) indicated that the conversion to glycolic acid was very rapid (minutes). Additional experiments are planned where oxaloacetic acid will be added to tissue extracts (early CDHs) to determine if the conversion to oxalic and acetic acids does, in fact, occur.

Initial tissue surveys indicated that the common, odoriferous amine indicators of decomposition, cadaverine, and putrescine would be useful biomarkers. Unfortunately, this was not the case in this study. While the concentrations of these compounds were quite abundant (>3000 ng/mg tissue) in some instances, the values (between corpses) were quite inconsistent as were the precursors of these compounds (lysine and ornithine). GHB was also a disappointment as a useful biomarker. Heart and kidney contained the most detectable GHB with concentrations in excess of 100 ng/mg tissue and while these tended to increase after the appearance of glycolic acid, they were inconsistent and did not correlate with glutamine, GABA or any other indicator. GHB was detected in low concentrations in deep muscle and brain and was virtually absent from liver tissue even though GABA and glutamine increased steadily. Vickers et. al, (14), showed that GHB can be metabolized into GABA once it crosses the blood-brain barrier. If this conversion does in fact occur in cadavers, it was neither a steady nor reproducible event.

While putrescine and cadaverine were not determined to be useful biomarkers, specific amino acids were significant PMI markers and were dependent on the tissue type (Table 3). Amino acids are small organic acids containing an amine (—NH₂) group and a carboxylic acid group (—COOH) and are the basic building blocks of proteins.

One of the interesting results to emerge from this study was the observation that every organ studied produced such a varied assortment of complex biomarker information. While the water content and assortment of cellular enzymes varies from organ to organ, the basic building blocks should be quite similar. During putrefaction, the abdominal organs (kidney, liver) are exposed to different bacterial populations than the thoracic organs (heart, lungs) and while this may produce varying results initially, it appears as if the tissue still exerts its “personality” long after decomposition has progressed to the point where the organs are no longer recognizable.

Model Design and Application

Since every death involves its own unique set of circumstances, the model was designed to take into account the many ways in which individuals perish. To accomplish this, the model was de-

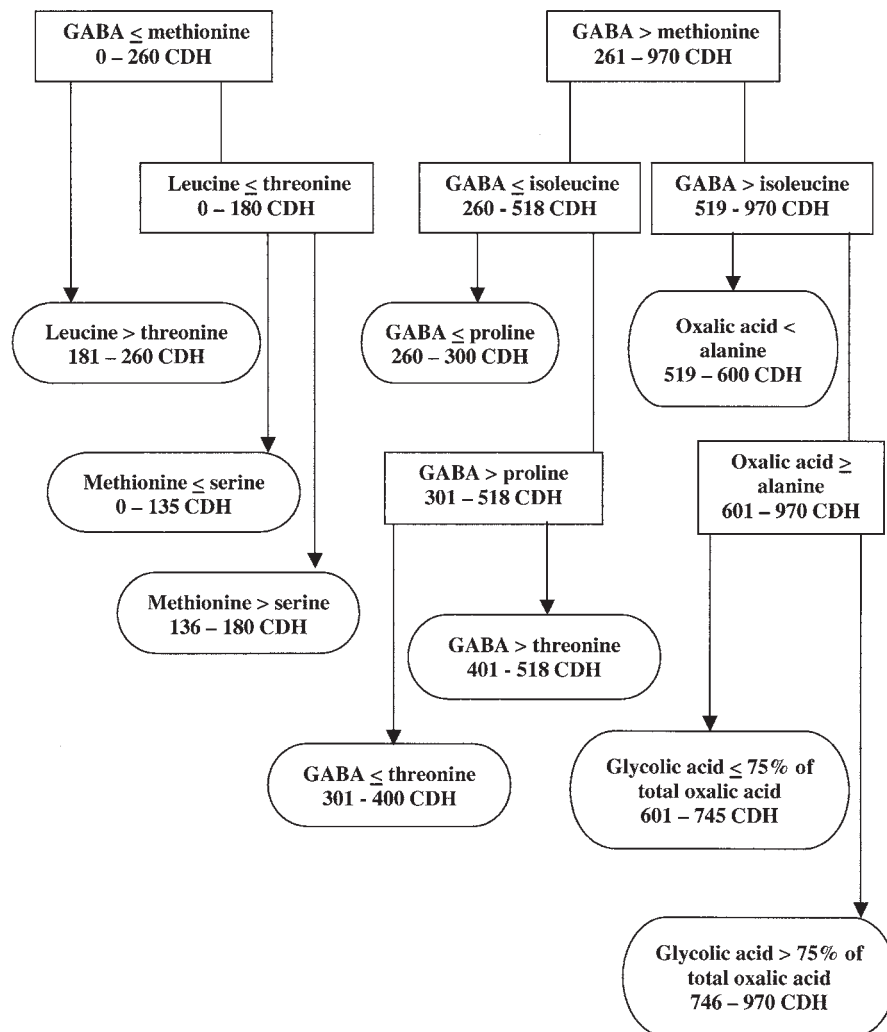


FIG. 5—Kidney (Potential CDH Range 0-970).

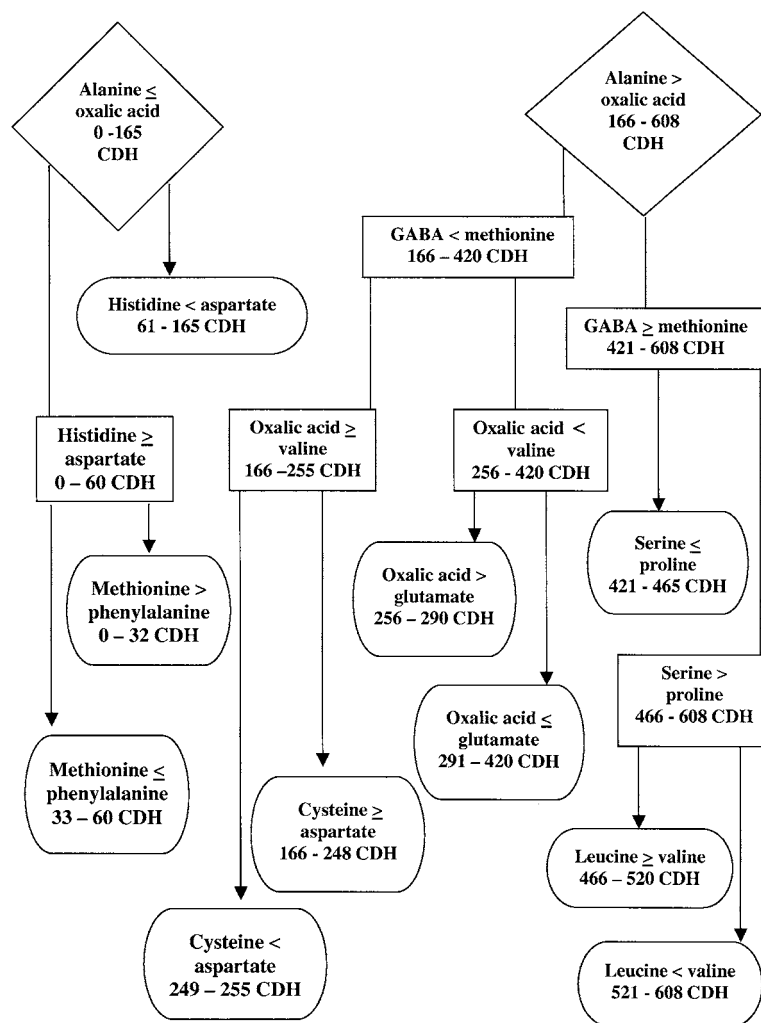


FIG. 6—Heart (Potential CDH Range 0–608).

veloped to encompass more than one indicator organ. For instance, if the individual's heart was damaged by trauma, there are four other organs from which to obtain useful data. The more organs used, the narrower the PMI becomes. Crossmatching PMIs from several organs can result in intervals as narrow as 5 CDHs—a time frame below the ability of the investigator to obtain reliable temperature data. This model also has the distinct advantage that additional information about the victim, such as weight, is not required since the model was developed based on ratios between the biomarkers and not absolute values. In fact, the amount of material processed for each organ becomes irrelevant since one is only concerned about whether or not the abundance of one biomarker is greater or less than another, but care must be taken not to exceed the solubility of the compounds of interest (Table 4). One potential disadvantage is that the model is organ specific. Uncertainties in organ collection (i.e., the wrong organ sampled or more than one organ sampled accidentally) could result in highly erroneous intervals. Therefore, you must be confident that you apply the correct model to the correct organ. Sample processing is also a critical factor. No attempt was made to stop enzymatic activity in the tissue samples once processing had begun. This was done intentionally to avoid adding possible compounds that may have interfered with the derivatization or analysis. Since many enzymatic systems are acti-

vated upon grinding the sample, all procedures were performed on ice to minimize additional enzymatic effects. All samples were also analyzed as soon as possible after processing to minimize possible changes occurring in the samples. Finally, for model development, when a value is designated as being equal to another value, it must fall within 10% of that value to be grouped in that category (Figs. 1–5).

The model is used by noting the relative concentrations of key pairs of biomarkers for each tissue sampled and following the “CDH roadmap” in Figs. 1–5. The following examples illustrate the application of the model.

Applications: The following two cases, provided by the Knox County Medical Examiner's Office, have a known time of death and are being used to illustrate this PMI technique. If these were unknown cases, the CDH values obtained from this technique would be correlated to corrected temperatures at the scene to determine the PMI.

Case 1

A 28-year-old black male was found with multiple gunshot wounds (45 caliber handgun) to his chest, abdomen, and right thigh. Samples collected during autopsy 27 h after death occurred

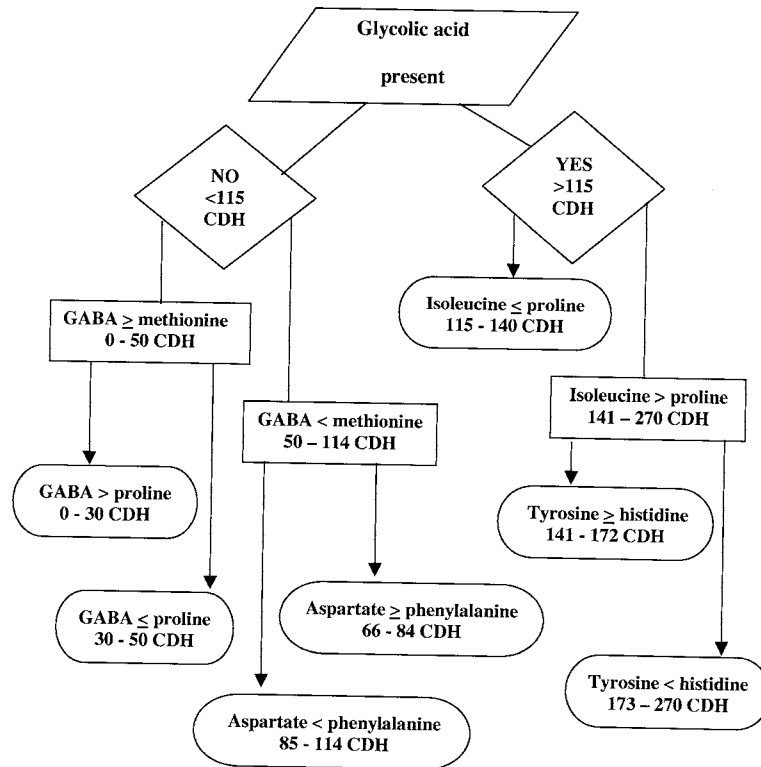


FIG. 7—Brain (Potential CDH Range 0-270).

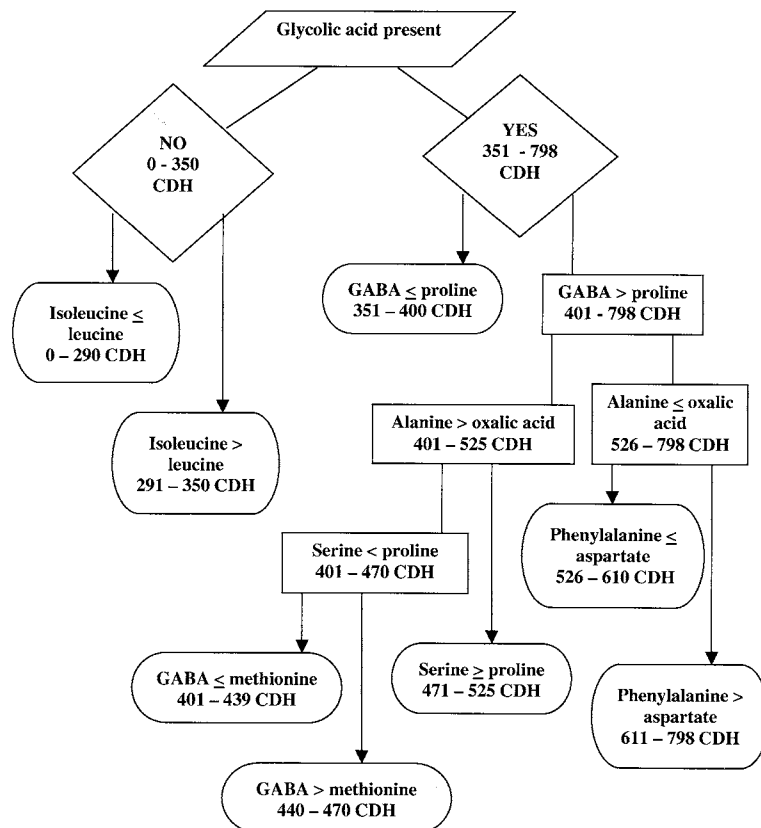


FIG. 8—Muscle (Potential CDH Range 0-798).

TABLE 4—Amino acid solubilities in water (25°C) (13).

Amino Acid	mg/mL
Alanine	166.5
Arginine	~150
Asparagine	~35
Aspartate	~5
Cysteine	Freely soluble
Glutamate	8.6
Glutamine	~47
Glycine	~250.0
Histidine	41.9
Isoleucine	22.3
Leucine	9.9
Lysine	Freely soluble
Methionine	18.2
Phenylalanine	29.6
Proline	1620.0
Serine	Soluble
Threonine	Freely soluble
Tryptophan	11.4
Tyrosine	0.45
Valine	83.4

TABLE 5—Application results for two test cases (results in ng/ml extract).

Biomarker	Case #1 Liver	Case #1 Kidney	Case #2 Kidney	Case #2 Liver	Case #2 Heart
Alanine	89.9	57.4	64.0	172.7	53.5
Aspartate	0.6	16.2	5.4	17.1	16.4
Cysteine	13.6	19.2	2.4	30.3	5.4
GABA	1.7	2.3	30.6	105.1	24.1
Glutamate	6.4	73.5	17.6	254.8	13.1
Glutamine	8.0	9.7	0.9	8.5	26.0
Glycine	19.6	27.9	13.5	29.2	39.5
Histidine	0.1	25.0	0.6	20.3	1.1
Isoleucine	14.8	29.4	31.9	93.9	32.2
Leucine	19.9	32.6	35.7	138.7	155.4
Methionine	10.2	19.5	19.5	59.7	75.0
Oxalic acid	111.4	272.1	17.2	43.9	16.7
Phenylalanine	12.4	18.9	17.0	60.7	57.1
Proline	14.4	24.4	41.1	49.0	62.0
Serine	7.4	20.7	6.0	72.8	24.0
Threonine	8.5	32.0	19.6	138.7	93.2
Tyrosine	13.5	51.3	4.1	53.2	19.2
Valine	20.4	37.8	47.9	23.7	130.3

included liver and kidney (brain was not collected, heart tissue was unusable, and muscle tissue would be of little value since this was a recent death). Following tissue processing, derivatization and analysis of the relevant biomarker concentrations were recorded (Table 5). Glycolic acid was not present in any of the samples.

Liver (Fig. 4)—since proline > GABA, glutamine > GABA and glycine is equal to valine (within 10%) we know that the CDH range is 0 to 98. Additionally, glutamate is greater than cysteine indicating a final CDH range of 0 to 49.

Kidney (Fig. 5)—GABA < methionine, leucine is equal to threonine (within 10%) and methionine is equal to serine indicating a CDH range of 0 to 135. Crossmatching the two organs indicates a final CDH range of 0 to 49. Additional organ tissues, had they been collected or usable, would have narrowed this time interval. Within

the first 12 h after death, this individual spent 5 h at 21°C and then was placed in a morgue cooler (4°C) with a resulting CDH of 12.5 (25/2). During the next 15 h he was removed from the morgue cooler (4°C) and spent 7 h at room temperature ~20°C with a resulting CDH of 12 (24/2). Combining these two 12 h CDH intervals results in a final CDH range of 24.5 CDH (12.5 + 12). This value is well within the estimated range of 0 to 49.

Case 2

A 61-year-old white male was found dead in his apartment (from heart failure) six days after he was last seen. During autopsy, samples collected included kidney, liver, and heart. Following tissue processing, derivatization, and analysis the relevant biomarker concentrations were recorded (Table 5). The apartment was kept at a constant 23.8°C. Calculating CDHs for every 12 h over the six day period (12 accumulations of 23.8°C) would result in 286 CDHs. The body was autopsied shortly after arrival at the morgue. Glycolic acid was present in all three samples.

Liver (Fig. 4)—Proline < GABA, oxalic acid > glycine and oxalic acid > valine provides a CDH range of 251–300.

Kidney (Fig. 5)—GABA > methionine, GABA < isoleucine, GABA < proline indicates a CDH range of 260 to 300.

Heart (Fig. 6)—alanine > oxalic acid, GABA < methionine, oxalic acid < valine, and oxalic acid > glutamate indicates a CDH range of 256 to 290. Cross matching provides a final CDH range of 260 to 290. This value again corresponds to the known PMI.

Acknowledgments

We gratefully acknowledge the University of Tennessee's Department of Anthropology for allowing us access to the Forensic Anthropology Research Facility, the United States Department of Energy, Office of Nonproliferation Research and Engineering, for supporting this research and to the following individuals who have continually supported this research endeavor: Dr. Dennis Wolf, Dr. Mike Burnett, Dr. Wayne Griest, Dr. Richard Jantz, Dr. Murray Marks, Dr. Steven Shubert, Vivian Baylor, and Dr. Michelle Buchanan. We also wish to thank Dr. Sandra Elkins from the Knox County Medical Examiner's Office for providing tissue samples and advice in collection methodologies.

References

- Gill-King H. Chemical and ultrastructural aspects of decomposition. In: Haglund WD, Sorg MH., editors. Forensic taphonomy: the postmortem fate of human remains. Boca Raton, FL: CRC Press, 1997;93–104.
- Clark MA, Worrell MB, Pless JE. Postmortem changes in soft tissues. In: Haglund WD, Sorg MH., editors. Forensic taphonomy: the postmortem fate of human remains. Boca Raton, FL: CRC Press, 1997;151–60.
- Coe JI. Postmortem chemistry update: emphasis on forensic application. Am J Forensic Med Pathol 1993;14:91–117.
- Vass AA, Bass WM, Wolt JD, Foss JE, Ammons JT. Time since death determinations of human cadavers using soil solution. J Forensic Sci 1992;37(5):1236–53.
- Perry WL III, Bass WM, Riggsby WS, Sirotkin K. The autodegradation of deoxyribonucleic acid (DNA) in human rib bone and its relationship to the time interval since death. J Forensic Sci 1983;28(2):423–32.
- Rulshrestha P, Chandra H. Time since death: an entomological study on corpses. Am J Forensic Med Pathol 1987;8:233–45.
- Keh B. Scope and applications of forensic entomology. Annual Rev Entomology 1985;30:137–54.
- Rodriguez WC, Bass WM. Insect activity and its relationship to decay rates of human cadavers in east Tennessee. J Forensic Sci 1983;28: 423–32.
- Haskell NH, Hall RD, Cervenka VJ, Clark MA. On the body: insects' life stage presence, their postmortem artifacts. In: Haglund WD, Sorg MH,

- editors. Forensic taphonomy: the postmortem fate of human remains. Boca Raton, FL: CRC Press, 1997;415-41.
10. Lehninger AL. Principles of biochemistry. New York: Worth Publishers, 1982.
 11. Knapp DR. Handbook of analytical derivatization reactions. New York: John Wiley & Sons, 1979.
 12. Edwards R., Chaney B, Bergman M. Pest & Crop Newsletter. 1987; 2:5-6.
 13. Windholz M, Budavari S, Blumetti RF, Otterbein ES, editors. The Merck index. Rahway, NJ: Merck & Co, 1983.
 14. Vickers MD. Gamma-hydroxybutyric acid. Int Anaesthesia Clin 1969;7: 75-89.

Additional information and reprint requests:

Arpad A. Vass, Ph.D.
Oak Ridge National Laboratory
1 Bethel Valley Road
P.O. Box 2008
X-10, 4500S, MS 6101, Room E-148
Oak Ridge, TN 37831-6101